STUDY OF SOLAR CELL WELDS

(NASA-CR-150887) STUDY OF SOLAR CELL WELDS Final Report (North Alabama Scientific and Engineering) 30 p HC A03/MF A01 CSCL 10A

N79-16354

Unclas
G3/44 43313

A Final Report for
Contract NAS8-33077

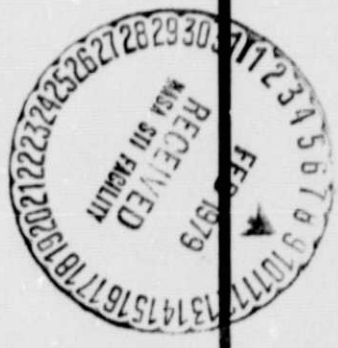

PREPARED
NOVEMBER 7, 1978

for

GEORGE C. MARSHALL SPACE FLIGHT CENTER
MARSHALL SPACE FLIGHT CENTER, ALABAMA 35812

by

Gary L. Workman
Principal Investigator

NORTH ALABAMA SCIENTIFIC & ENGINEERING CONSULTANTS, INC.
HUNTSVILLE, ALABAMA

NORTH ALABAMA SCIENTIFIC & ENGINEERING CONSULTANTS, INC.

P. O. Box 5124
Suite 105, Executive Plaza
4717 University Drive
Huntsville, Alabama 35805
Phone (205) 837-6940

STUDY OF SOLAR CELL WELDS

Gary L. Workman - Principal Investigator

November 7, 1978

Final Report for

Contract NAS8 - 33077

prepared for

George C. Marshall Space Flight Center

Marshall Space Flight Center, Alabama 35812

AP29-F	(1)
AS24D	(3)
AT01	(1)
EM63-13	(1)
EH13/Woodis	(3)

ABSTRACT

The thermal imaging technique has been evaluated for its capabilities in the nondestructive evaluation of solar cell welds. The temperature and spatial resolution of state of the art instrumentation is sufficient for both qualitative and quantitative determination of the quality of solar cell welds. The addition of color digitized thermography enhances the NDE aspects of the thermographic display and allows easily computerized testing procedures. For automated testing systems an accurate correlation of weld quality with temperature profiles of the welds needs to be performed. In comparison, the holographic technique is complementary with the thermal imaging technique except that the holographic analysis appears to be more quantitative at the present time. However the thermal imaging approach is much more versatile in overall NDE capabilities.

TABLE OF CONTENTS

INTRODUCTION

The requirement for quality control testing of solar cell arrays which are to be packaged for space flight has shown that there is very little experimental data available on the testing of solar cell arrays, particularly with respect to the quality or reliability of the weldments of the cells. In order to provide a starting place for the evaluation of nondestructive testing techniques which can be used for quality control in the fabrication of the solar cell arrays, we have performed several experiments using holographic interferometry and infra-red imaging as nondestructive testing techniques. The previous work in this area, performed on contracts NAS8 - 32126 and NAS8 - 32468, demonstrated that both qualitative and quantitative information about the solar cell welds were obtainable with the real time holographic interferometric approach and that at least a qualitative analysis was possible with thermal imaging approaches. The results obtained in these studies also indicated that the thermal imaging technique, which will be discussed in more detail in this report, could be an extremely useful qualitative inspection technique for a large solar cell array. The usefulness of the technique for a quantitative measure of the weld bonding strength was questionable due the question of having sufficient resolution to identify temperature differences across the weld itself. This question has been resolved in the present study, in which we have looked more closely at the capabilities

of a commercial infra-red imaging system in order to demonstrate the quantitative capabilities of the infra-red imaging technique.

A number of advantages can be given for using either the holographic interferometric technique versus the thermal imaging technique; however in the overall objective of providing an automated quality control inspection capability, the more easily automated thermal imaging system would probably be preferred. Our studies to date indicate that both techniques tend to complement each other to some degree. Since we have described the holographic nondestructive testing results in the previous contract reports, we will not discuss those results in this report, except where we need to provide some comparison between the two techniques.

WORK STATMENT

North Alabama Scientific & Engineering Consultants, Inc. proposed to provide the personnel, facilities, and materials in order to perform the following tasks.

Task 1. Set up a demonstration thermal imaging test which will provide the necessary data for determining bond area of solar cell welds provided by the government.

Task 2. Evaluate the results of the proposed thermal imaging tests and provide a recommendation of which nondestructive testing method will be the most cost effective for solar cell NDE.

Task 3. Provide engineering data which substantiates the above recommendations in the form of a final report with appropriate graphs, drawings and photographs.

EXPERIMENTAL RESULTS

The same solar cell module as used in the two previous studies was used for this work. Also the same technique of loading the solar cells by forward biasing the pn junction was used to generate the thermal excitation for these tests.A UTI-Spectrotherm Model 900 Industrial Thermal Imaging System with the isotherm option and the color quantized thermographic capability was used to obtain the thermal images presented in this report. The emphasis of this work has been to utilize these options and demonstrate the types of information which can be obtained for NDE applications. In order to comprehend the information contained in the thermal photographs presented here it is necessary to define a few of the terms used in the explanation.

The thermal imaging technique is applicable to the nondestructive evaluation of solar cell welds only if the weld quality information can be transformed into an observable surface temperature effect. The three categories which would be of interest for the quality requirements are total nonbonds, bad welds and good welds. In the analysis presented here we will assume that a good weld will have the strongest bond, provide a larger bonding area, and provide the lowest resistance to current flow among the three possibilties. In the present analysis then we provide a thermal excitation at the weld itself and then evaluate the thermal images for their information content. In

any analysis of this type we can look for two types of information, a qualitative type which can be used for an overall indication of nonbonds in the array, but in general can not differentiate a good weld from a bad weld and a quantitative type, which can differentiate between a good weld and a bad weld. The data obtained in this study will be presented in the form of thermograms, which were taken with the instrument described above in its normal operating procedure.

A good example of qualitative evaluation is given in Figures 1-4. This thermograph was obtained by loading the solar cell array with the various currents given and observing the effect of these current loads from the front of the cell. Dring loading, the cells heat up, as any resistive load would, and these temperature levels are indicated along the bottom. Notice that several temperature levels are obtained depending upon the amount of current flowing through the array. Several significant observations are apparent in these figures. First, the hottest features are white and the dark features are colder, hence we can automatically reason that the dark cell in the middle left is dead; i.e. no current flows through that cell, even at the largest current levels. The obvious choice of conditions is that there is a nonbonded weld on that particular cell. Since these thermographs show the temperature of the front surface, we cannot discern which weld is bad, but that there is at least one bad weld in the array. We do have indications that several of the

cells in the lower right hand corner also are not bonded very well. A visual analysis of the solar cell welds on these two cells indicates that the left most weld of the centrally located cell was nonbonded on the far left weld. Similar analysis of the two cells on the lower right proved to have a similar nonbonded condition. One can also evaluate how the surface temperature of each solar cell varies with temperature and determine some measure of the electrical properties of each cell. A good array should be fairly uniform; so this particular array does have a number of bad cells or welds, and the bad cells are easily discerable. The only difference between Figures 3 and 4 is the position of the scan line which provides some measure of quantitative temperature profiles. The ability to obtain temperature profiles with scan lines will prove to be useful in automated testing applications.

In order to obtain information pertinent to the weld quality itself it is necessary to look at the weld side of the array. Figure 5 shows an overall view of the array still using 1 ampere to load the cells. Notice that the kapton sheet is more emissive (looks hotter) than the welds. This may be due to the infra-red emission of the solar cells themselves, which have been heated up by the current even though the kapton does attentuate the radiation somewhat or the emission may be from the solar cells themselves. This question is answered later when we consider the results of the color digitized thermograms.

The temperature profile at the bottom of the figure shows the difference in temperature between the metal welds and the kapton backing. The dead cell in the photograph does show up again as a dark region, so that this type of interpretation can be made from either side of the array. This particular thermal image represents a single scan and does provide a noisy temperature profile. In particular it is not too clear whether or not we can observe temperature differences across the welding pads themselves. Figure 6 shows the same experiment with an averaged thermograph of 25 scans. The major improvement is in the representation of the temperature profile, which now shows a temperature gradient across the weld pads themselves. This is one of the features which will be required for weld quality interpretation.

The welds which have been formed are in general bonded in the middle of the pad, with the outer edges unbonded to any other surface. Therefore the temperature profile across the welding pad itself is hotter in the weld region and cooler away from the center. This phenomenon was observed in the holographic study by fringe displacements at the bonding area and lesser fringe shifts away from the bonding area. The same information can be obtained with the thermal imaging tests by use of the scanned temperature profiles. The thermograph in Figure 6 does show one approach to this requirement. Another method which is available is to display in either white or black those temperatures which fall in a

narrow temperature range. This approach, shown in Figures 7 and 8, is called the isotherm technique. In the present instrumentation the operator turns a pot which changes the isotherm level from the minimum temperature level through to the maximum temperature level continuously along a ramp. Those areas falling into the "window" are enhanced areas and are easily discernable on the thermograph. Both polarities are shown and the information about which parts of the welds are hotter is there, but the field of view is too large for human eyes to discern which welds are not good welds.

One approach would be to magnify the images of the welds in order to make a visual interpretation more possible. This is shown in Figures 9 and 10 in which we have partitioned the field of view into four quadrants and display each quadrant at a time. Note that this is the same thermal image as in Figures 5 through 8, we are just displaying the data differently. Another point to remember is that we have not improved the resolution of the original image, we have merely made the images on the screen bigger. The digital nature of the image is apparent now, since we now see the squared pixels in the images. Further information can be obtained using the isotherm scans as shown in Figure 11. Notice that there is a difference in temperature between the outer and inner portions of the welds. In this particular scan the outer edges are cooler as would be expected.

Greater magnification can be obtained through the use of a

germanium lens which can be attached to collecting optics. The image formed this way is actually magnified and is shown in Figures 12-15, as quadrant displays. Notice that in these thermographs the information about the temperature gradients across the welds is obtained. We did not have any source of actual bond strength information to correlate the thermal patterns with a particular weld quality so that the true quantitative evaluation cannot be performed with these images. The temperature gradients observed across the weld indicates that the resolution is sufficient for quantitative analysis. Also the data obtained in the scans is available in digital format, which is easily used for computer controlled interpretation. A disadvantage of the present system is that the present system utilizes the manually controlled pot for the isotherm scan, which makes the present interpretation difficult because we do know actually what temperature level is being enhanced. However this feature would be easily automated with computer control and thus allow automated interpretation.

The thermal images presented above use shades of gray in order to show contrast across the images. Another approach is to use color digitized thermography and to let the temperature differences be represented by color differences. This approach is shown in Figures 16-21, where the temperature range is divided into ten units, each shown as a unique color. In this representation the hotter regions are shown in blue, while the

cooler areas are seen as brown. One useful feature is that the color scale is shown on the display (and in the photograph) so that the actual temperature values are available to the operator. Figures 15 and 16 show similar experiments as performed with the black and white images previously, but demonstrate the amount of detail which can be obtained from a color representation. In some ways the display can provide too much detail for a human being to comprehend all the features, but fortunately the solar cell images do not become too crowded. Also with the color displays the four quadrant representation can be used to isolate particular scenes on the solar cell array. Note that both these figures show the dead cell has some emissivity and that the welds themseves have lower emissivity than the kapton sheet does. In addition the thermal images do not outline the cells exactly, indicating that the thermal patterns we have been using for solar cell information does come from the heating up of the kapton sheet and not directly from the back of the solar cells.

A useful feature of the digitized color display is the memory mapped information storage. As indicated earlier Figure 17 shows an example of the improved visibility of certain features with the four quadrant display and Figures 18-21 shows an extremely useful capability of this technology. A whole display can be stored into one of the quadrants and then all four quadrants can be displayed simultaneously. For example we have an unloaded array for Figure 20, in which no current is flowing.

Due to the emissivity of the surfaces some color variation is still observed. Figure 19 shows the same scene with a current of 750 milliamperes flowing through the cells. Note that there is more color variation across the array and the image looks more like Figure 16. Upon subtracting the background (Figure 20) from Figure 19, we obtain the display shown as Figure 21. In particular notice how dark the dead cell has become and the increased amount of color variation in the scene. In essence we have been able to compensate for the different emissivities of the surfaces by subtracting out the ambient emissivities. In case the other images were not remembered by the operator who is responsible for the quality testing, all can be displayed simultaneously as seen in Figure 18. These useful features provides us with temperature information which is independent of the materials being tested. Also this information is all easily handled with computer control with no problem.

CONCLUSIONS

The temperature information presented in the thermograms show that thermal imaging techniques are applicable to solar cell welds and may be used for the nondestructive evaluation of the welds. The qualitative NDE capabilities of thermal imaging are apparent from the commentary presented with the photographic data. The quantitative evaluation of the welds has not been completed, since in this particular study we were not able to provide a bonding strength test with the thermographic information. The need for a quantitative capability is obviously going to be very high in large production environments of space qualified solar cell arrays. The interpretation of the thermal images presented here is fairly straight forward and would be easily adapted for NDE inspection without a large amount of personnel training. In comparison with the holographic study performed previously the thermal imaging technique provides a much simpler inspection procedure, without requiring motion restrictions or fringe interpretations. We have found that persons not familiar with holographic interpretation are extremely dubious of fringe interpretation. Even though surface motion due to temperature differences arises from the same effect as the thermographic display, the thermal images are more easily understood by untrained personnel. The overall capability of the thermal imaging process as described in this report suggests that this technique has more range with the different types of testing

which might be required for the solar cells. One question which has not been answered in this study is which technique provides the most sensitive temperature probe for testing small objects, such as the solar cell welds. Since the holographic information is originally stored on a photographic plate and the unit of measure is around 514.5 nanometers we obtain an extremely fine tool for measuring surface detail or surface displacements. The fringes which appear upon surface displacements have been transformed from the temperature domain into the physical domain through the coefficient of expansion of the material. Therefore, depending upon the coefficient of expansion of the material and the temperature gradient through the sample, the holographic interferometric inspection can provide a very sensitive test. However we are not able to provide a number for this sensitivity since it is materials dependent. Moreover the ability to subtract out background emissivities improves the detectability of temperature changes with thermal imaging, which allows the observer to identify the temperature differences due to a loading effect rather than fringes appearing on a hologram. Hence we feel that the two techniques are comparable as far as their applicability to the inspection of solar cell welds. The holographic results from the previous study does indicate that to date the holographic testing is quantitative in being able to determine extent of bonding in the solar cell welds. The type of data obtained with the thermal imaging technique does not lend

itself to be as easily quantitative without some external correlation such a pull test. The thermal imaging technique is certainly a simpler test and with the improved technology provides a much simpler process to interface to a computer for an automated inspection procedure. It is still felt that both techniques have their merits and can complement each other as nondestructive testing tools.

ACKNOWLEDGEMENTS

I wish to thank Dr. James Willis for his assistance in performing the thermal imaging tests at UTI-Spectrotherm, Inc. and Carol Y. Workman for assistance in the preparation of this report.

Figures 1-4. Qualitative aspects of thermal imaging can be seen by observing front of solar cell array while loading with the following currents:

1. 250 milliamperes
2. 500 milliamperes
3. 1 ampere
4. 1 ampere

Note the temperature profile indicated by the scan line across the array. The temperature profile is given at the bottom of the photograph.

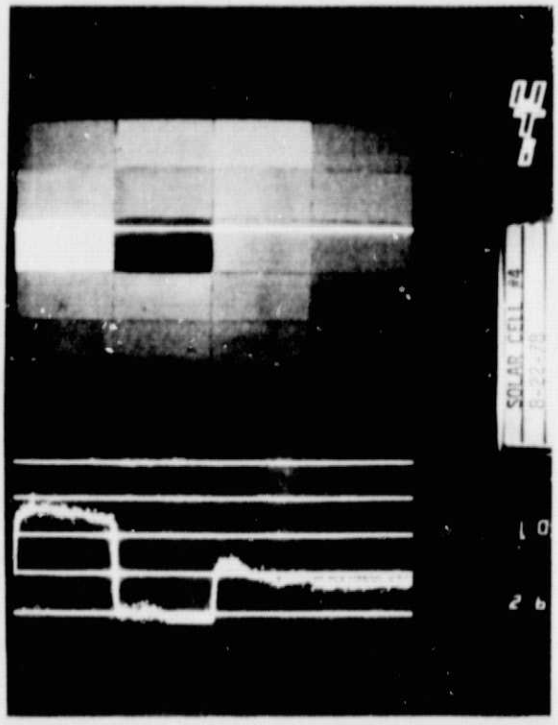

(1)

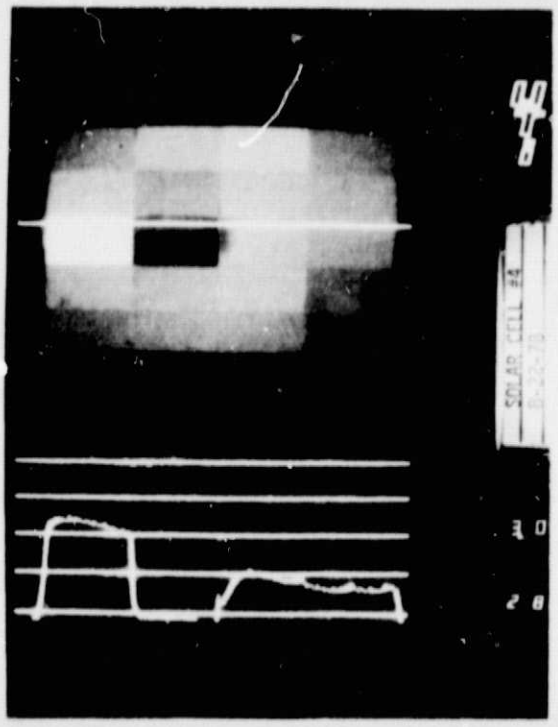

(2)

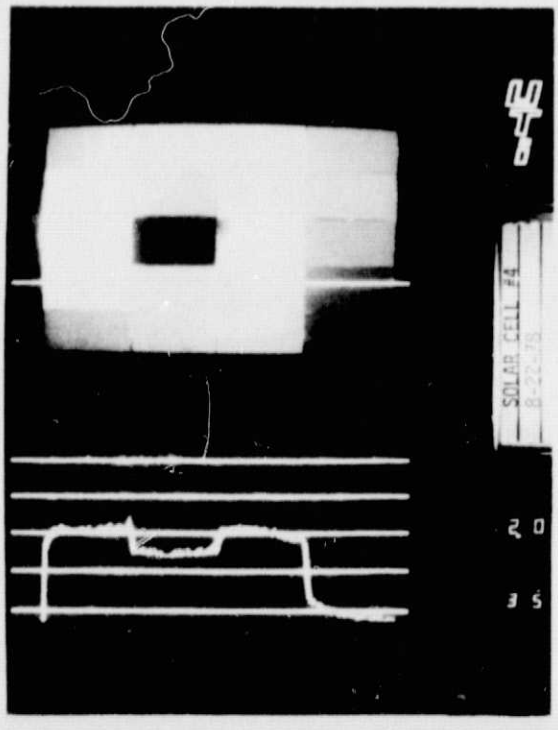

(3)

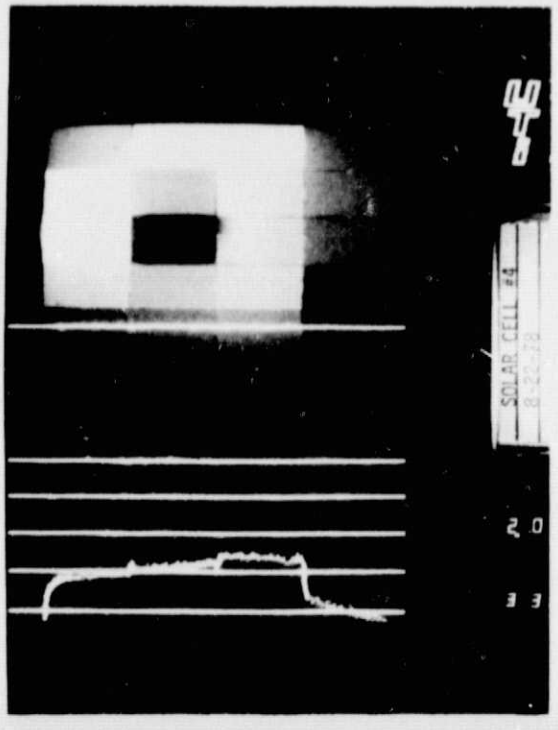

(4)

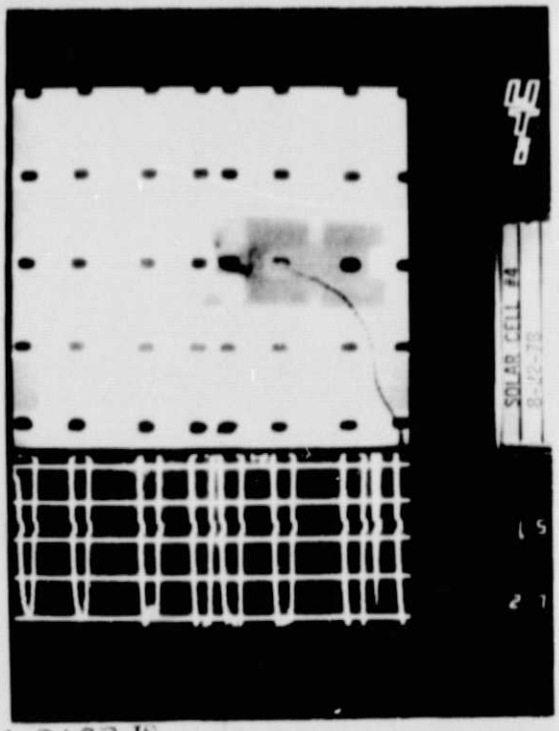

Figure 5. Thermal image of solar cell array from the weld side at 1 ampere load current.

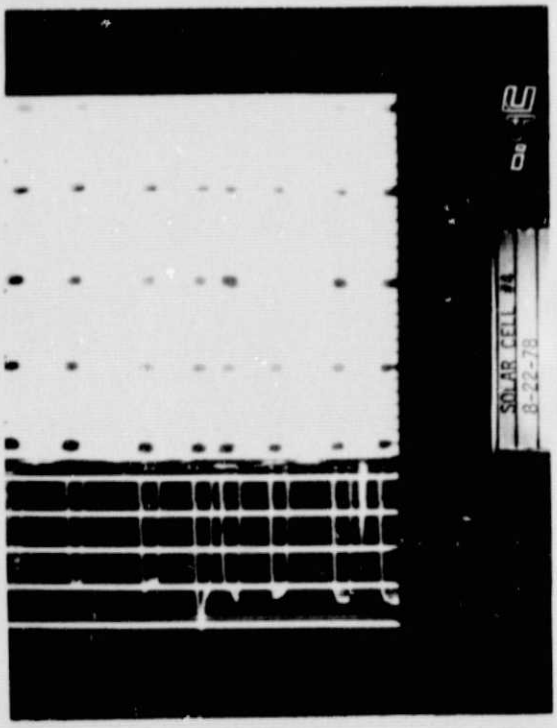

Figure 6. Same parameters as above except that photograph shows average over 25 scans. Note temperature profile across weld itself.

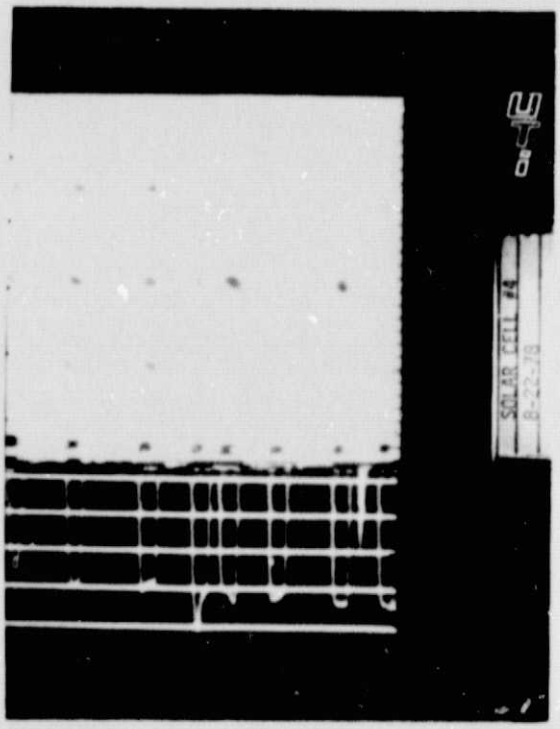

Figure 7. Same parameters as Figure 6 except isotherm feature is employed in this photograph. See text for explanation of this feature.

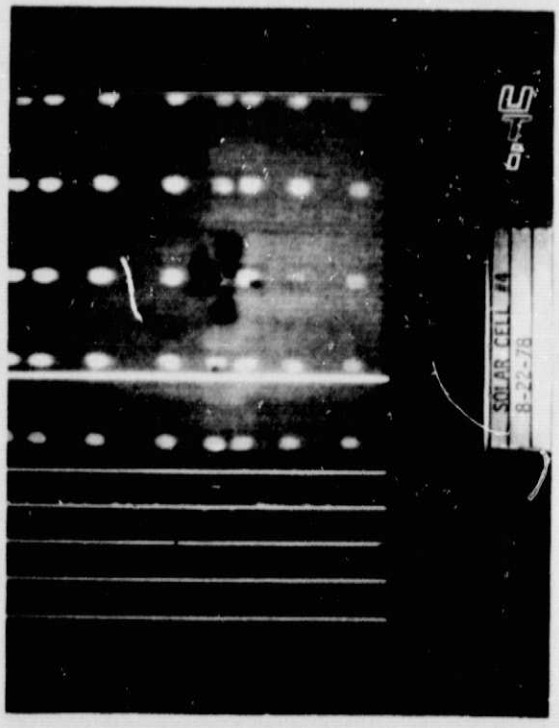

Figure 8. Same parameters as above except that reverse polarity on temperature display. Now the hotter surfaces are dark.

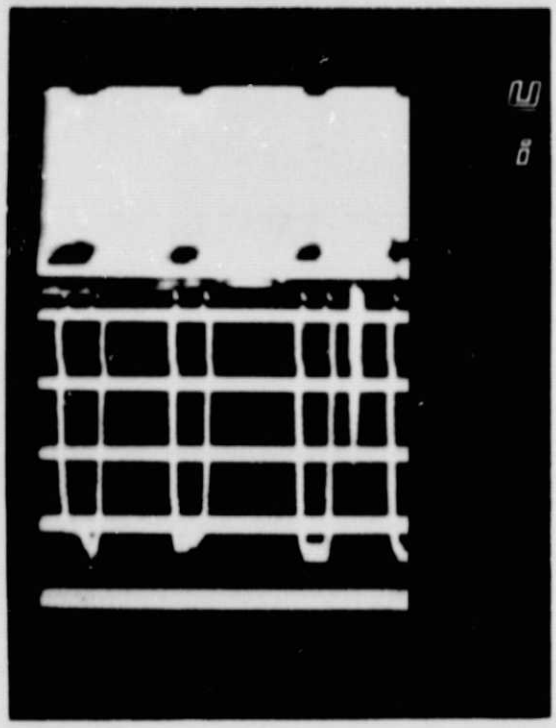

Figure 9. Same data as obtained in Fig 6, except that lower right quadrant fills screen.

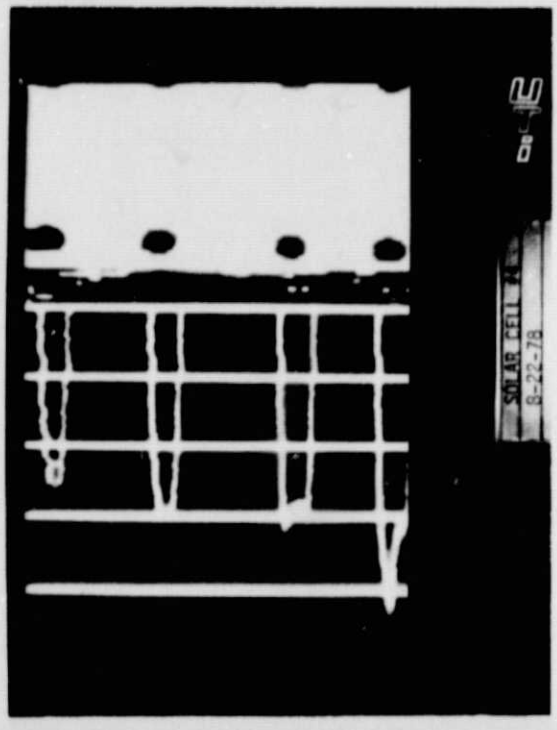

Figure 10. Same as above, except now lower left quadrant fills screen.

Figures 11 - 13. Several examples of the magnified images obtained with a germanium lens in the optical path and use of the four quadrant display.

11. Isotherm display with reverse polarity at 500 milliamps. Display shows lower left corner.

12. Similar display with germanium lens in position.

13. Same as Figure 12, with positive polarity.

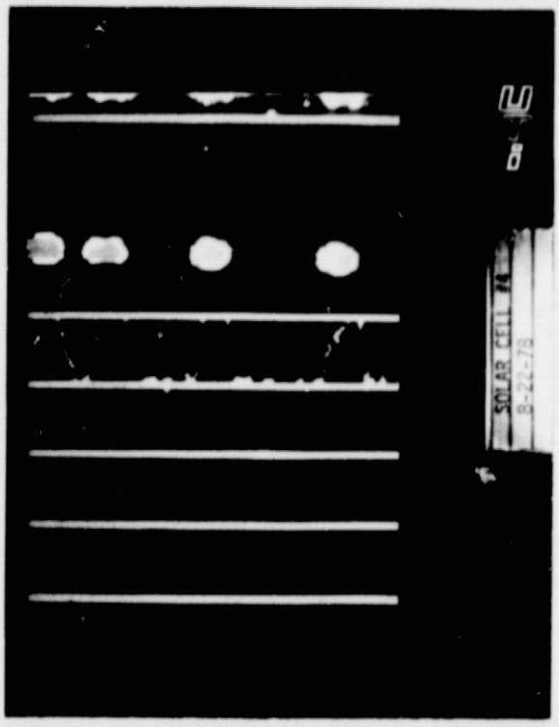

(11)

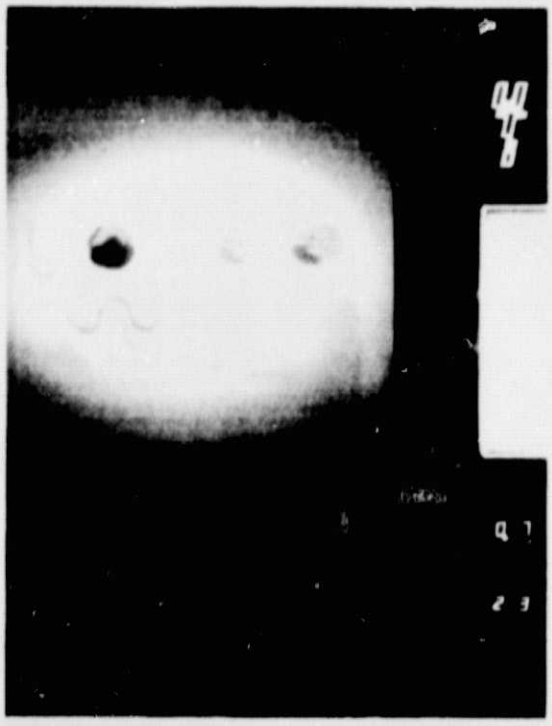

(12)

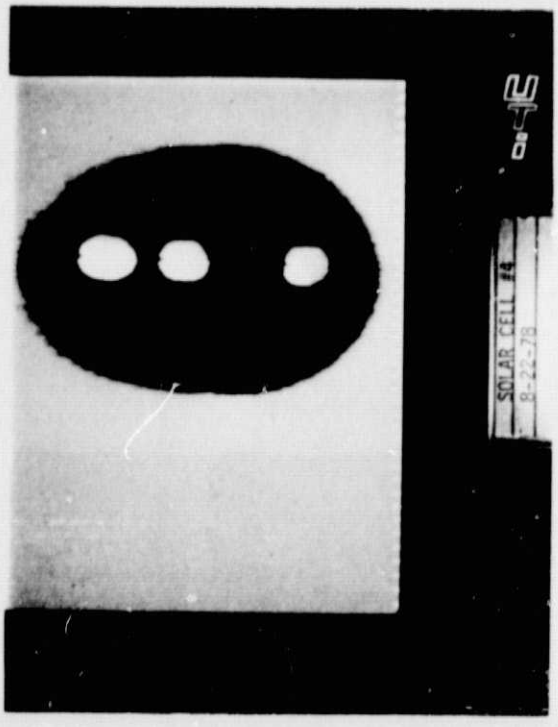

(13)

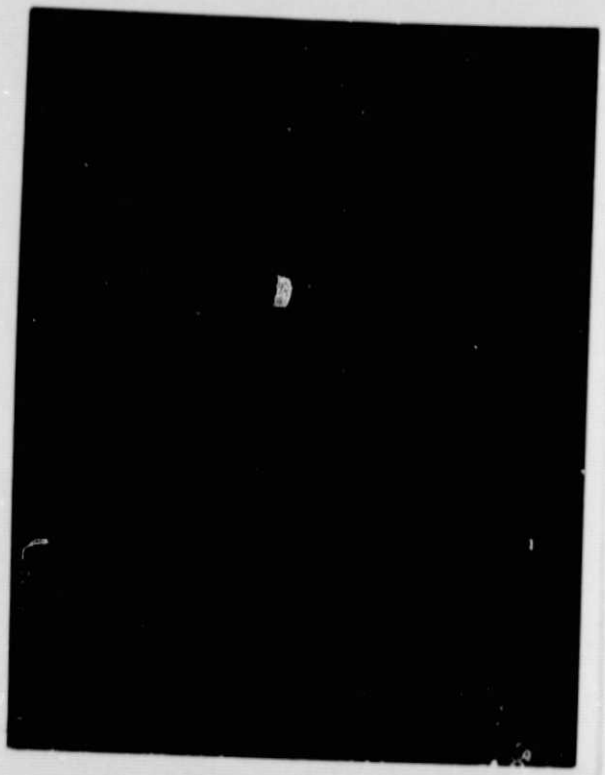

Figure 16.
Digitized color thermograph of solar cell module with 500 milli-amperes loading.

Figure 17.
Quadrant display of digitized color thermograph positioned to show features in center of array.

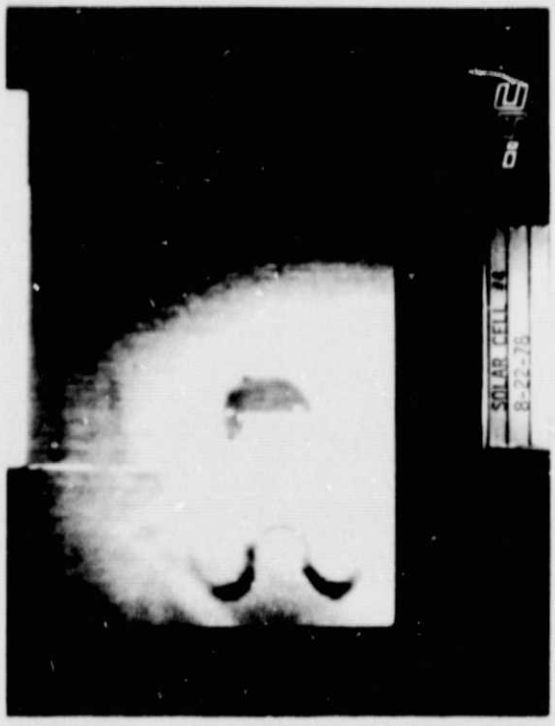

Figure 14. Maximum magnification using germanium lens and four quadrant display. Positice polarity with isotherm display.

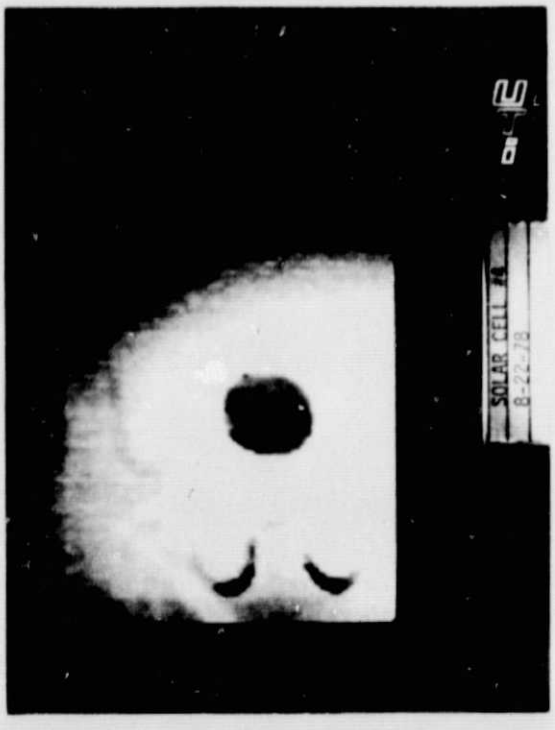

Figure 15. Same parameters as in Figure 14, reverse polarity display.

Figures 18-21. Color thermographs showing composite capability of digitized color technique

Figure 18. Composite view of the following displays:
a. upper left - 750 milliamperes current
b. upper right - difference between loaded and unloaded cells
c. lower left - unloaded cells
d. lower right - not identified

Figure 19. Cells loaded with 750 milliamperes.

Figure 20. Cells with no load.

Figure 21. Difference display between loaded and unloaded cells.

(18)

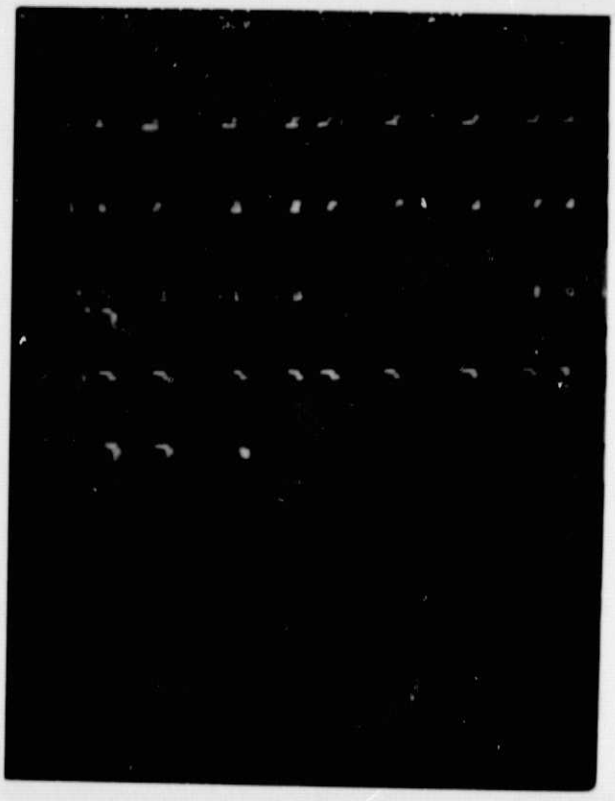

(19)

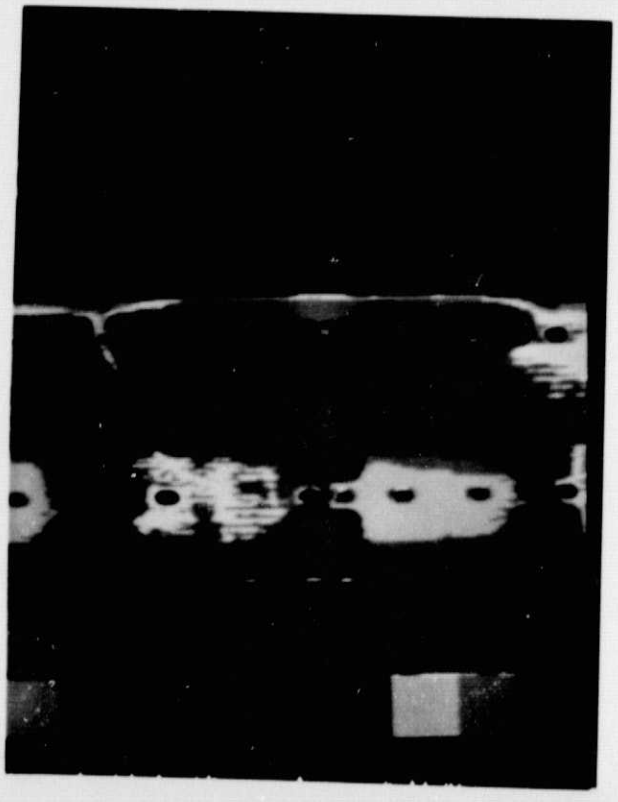

(20)

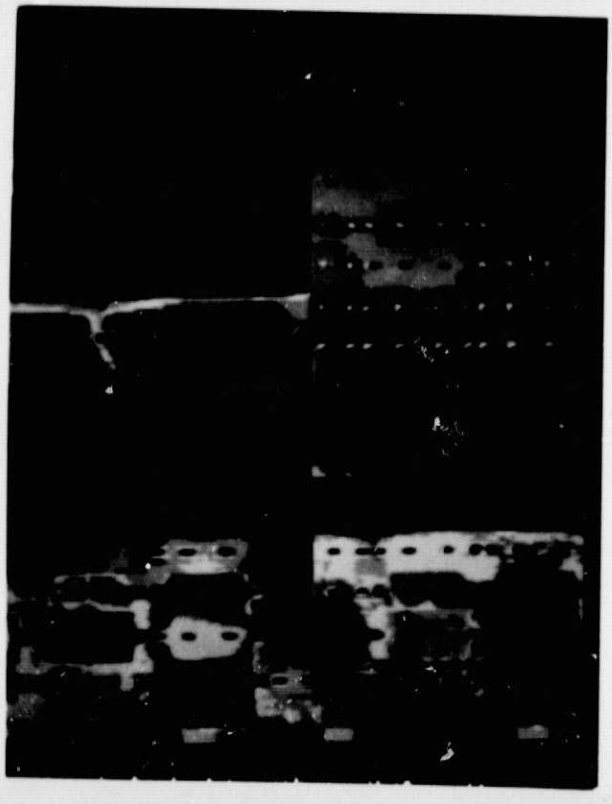

(21)